State-Independent Experimental Test of Quantum Contextuality with a Single Trapped Ion

Xiang Zhang,[1] Mark Um,[1] Junhua Zhang,[1] Shuoming An,[1] Ye Wang,[1] Dong-ling Deng,[1,2] Chao Shen,[1,2] Lu-Ming Duan,[1,2] and Kihwan Kim[1,*]

[1]*Center for Quantum Information, Institute for Interdisciplinary Information Sciences, Tsinghua University, Beijing 100084, People's Republic of China*

[2]*Department of Physics, University of Michigan, Ann Arbor, Michigan 48109, USA*

(Received 11 September 2012; published 11 February 2013)

Using a single trapped ion, we have experimentally demonstrated state-independent violation of a recent version of the Kochen-Specker inequality in a three-level system (qutrit) that is intrinsically indivisible. Three ground states of the $^{171}Yb^{+}$ ion representing a qutrit are manipulated with high fidelity through microwaves and detected with high efficiency through a two-step quantum jump technique. Qutrits constitute the most fundamental system to show quantum contextuality and our experiment represents the first one that closes the detection efficiency loophole for experimental tests of quantum contextuality in such a system.

DOI: 10.1103/PhysRevLett.110.070401 PACS numbers: 03.65.Ud, 03.65.Ta, 32.50.+d, 37.10.Ty

It is a long-standing debate whether quantum mechanics gives a complete description for all the properties of physical systems. In the world view of classical reality, the measurement outcomes on physical properties are noncontextual, i.e., predetermined independent of other compatible measurements that can be performed simultaneously, while in quantum mechanics measurements are contextual. Kochen, Specker, and Bell proved that quantum mechanics and any theory based on noncontextual classical reality give conflicting predictions [1,2]. The conflict is rooted in the structure of quantum mechanics and independent of the states of the system. This conflict was later reformulated as experimentally testable inequalities, in general referred to as the Kochen-Specker (KS) inequalities. The conventional Bell inequalities can be considered a special type of the KS inequalities, where the contextuality is enforced by nonlocality. While Bell's inequalities can be violated only by entangled states, the violation of the KS inequalities in principle can be observed for any state of the system.

A number of recent experiments [3–6] have demonstrated the Kochen-Specker inequality for two qubits [7–9], using photons, ions, neutrons, or nuclear spin ensembles. In particular, the experiment [3] closes the important detection efficiency loophole for experimental tests of quantum contextuality on two qubits using trapped ions. On the other hand, it is known that two qubits are not the simplest system to show quantum contextuality. A single three-level system, called a qutrit, is the most fundamental system manifesting the conflict between quantum mechanics and noncontextual hidden variable theory. The test of the KS inequality with qutrits is of special interest for several reasons. Firstly, a qutrit is the simplest system to show quantum contextuality. Second, a violation of the KS inequality in a three-level system would imply its violation in higher dimensions with $d > 3$; however, the reverse is not true. In this sense, it is more fundamental to test the KS inequality in the qutrit system. Finally, the qutrit system is intrinsically indivisible with no tensor product structure for its Hilbert space and thus has absolutely no entanglement. A violation of the KS inequality in qutrits clearly shows that quantum contextuality is not based on entanglement or particular quantum states but rooted in the fundamental structure of quantum mechanics.

Experimental tests of quantum contextuality with indivisible qutrits only became possible very recently, with significant improvement of the KS inequalities for qutrit systems. A version of the KS inequality for qutrits was proposed in Ref. [10] using five measurement settings; however, this version of the KS inequality requires us to prepare the system in a particular quantum state and thus is not state independent. A significantly simplified state-independent version of the KS inequality was proposed recently in Ref. [11] using 13 measurement settings, and 13 has been proven to be the minimum number of settings required for tests of quantum contextuality in a qutrit system [12]. On the experimental side, for a qutrit system, the violation of state-dependent KS inequality was first observed in Ref. [13] and the state-independent experimental test of quantum contextuality was just reported in Ref. [14]. Both of these experiments use single photons to represent qutrits and thus are subject to the detection efficiency loophole because of the low detection efficiency of photons as well as the post-selection technique required in this kind of experiment.

In this Letter, we report the first experimental test of quantum contextuality for a qutrit system that closes the detection efficiency loophole. We use three ground states of a single trapped ion to represent a qutrit. The violation of the KS inequality for a qutrit is only about a few percent even for a perfect system. We use high-fidelity quantum gates based on microwave operation to rotate the

measurement bases and a two-step quantum jump technique to distinguish the qutrit states and measure all the required correlation functions with a high detection efficiency. The KS inequality is observed to be violated for all the 12 different quantum states.

The basis vectors for a qutrit are denoted by $|1\rangle$, $|2\rangle$, $|3\rangle$. The 13 observables in the KS inequality take the form of $A_i = I - 2V_i$, where V_i is the normalized projection operator onto a vector $|v_i\rangle = a|1\rangle + b|2\rangle + c|3\rangle$. The 13 corresponding vectors $|v_i\rangle$ are displayed in a three-dimensional Hilbert space as shown in Fig. 1(a), with real values for the coefficients (a, b, c), which are general enough for our purpose. In Fig. 1(b), an edge $(i, j) \in E$ indicates the orthogonal relation of the projectors $V_iV_j = 0$, where the corresponding A_i and A_j are compatible observables. In total, there are 24 compatible pairs (A_i, A_j) represented by the 24 edges in Fig. 1(b). An improved version of the KS inequality for a qutrit system takes the form [15],

$$\langle \chi_{13} \rangle = \sum_{i \in V} \mu_i \langle A_i \rangle - \sum_{(i,j) \in E} \mu_{ij} \langle A_i A_j \rangle - \sum_{(i,j,k) \in C} \mu_{ijk} \langle A_i A_j A_k \rangle \leq 25, \quad (1)$$

where $\langle \cdots \rangle$ denotes the average of measurement outcomes, $\mu_i = 1$ for $(i = 1, 2, \ldots, 9)$, $\mu_i = 2$ for $(i = 10, \ldots, 13)$, $\mu_{ij} = 1$ when (i, j) are in the triangles $\{(1, 4, 7), (2, 5, 8), (3, 6, 9)\}$, and $\mu_{ij} = 2$ otherwise. In Eq. (1), C denotes the set of four triangles in Fig. 1(a), and $\mu_{ijk} = 3$ when $(i, j, k) \in \{(1, 4, 7), (2, 5, 8), (3, 6, 9)\}$ and 0 otherwise. This inequality can be derived through an exhaustive check of all possible assignments of values ± 1 to the 13 variables. In quantum mechanics, one finds $\chi_{13} = (25 + 8/3)I$ when A_i are identified with the qutrit observables given in Fig. 1(a), which clearly violates the inequality (1) independent of the system state.

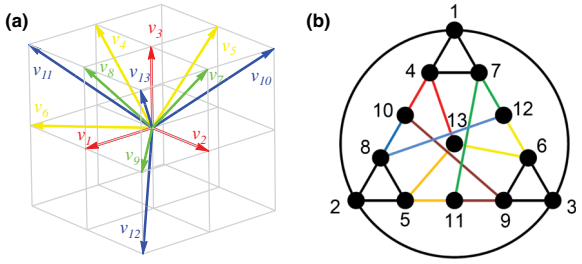

FIG. 1 (color online). Observables and compatibility relations for the state-independent KS inequality for a qutrit system. (a) The 13 observables are represented as vectors in a three-dimensional space. $|v_i\rangle$'s are specified as $|v_1\rangle = (1, 0, 0)$, $|v_2\rangle = (0, 1, 0)$, $|v_3\rangle = (0, 0, 1)$, $|v_4\rangle = (0, 1, -1)$, $|v_5\rangle = (1, 0, -1)$, $|v_6\rangle = (1, -1, 0)$, $|v_7\rangle = (0, 1, 1)$, $|v_8\rangle = (1, 0, 1)$, $|v_9\rangle = (1, 1, 0)$, $|v_{10}\rangle = (-1, 1, 1)$, $|v_{11}\rangle = (1, -1, 1)$, $|v_{12}\rangle = (1, 1, -1)$, and $|v_{13}\rangle = (1, 1, 1)$. (b) The compatibility graph between 13 observables. The nodes represent the 13 vectors $|v_i\rangle$ and the 24 edges show the orthogonality or compatibility relations. The experimental realization and joint measurements of the 24 orthogonal observables are described in Table I and Fig. 2(c).

For a more strict hidden variable model that is required to preserve the algebraic structures of compatible observables, one can derive another inequality [11],

$$\langle \chi_4 \rangle = \sum_{i=10}^{13} \langle V_i \rangle \leq 1. \quad (2)$$

This inequality is only valid under the additional assumptions of the product rule and the sum rule [11], so it is logically weaker but easier to be violated in experiments. Quantum mechanics predicts $\chi_4 = (4/3)I$, so the inequality (2) is violated quantum mechanically with a significant margin.

We test the KS inequalities (1) and (2) using a single trapped $^{171}Yb^+$ ion in a four-rod Paul trap with the setup similar to the one described in Ref. [16]. The basis vectors of a qutrit are represented by the three hyperfine levels of

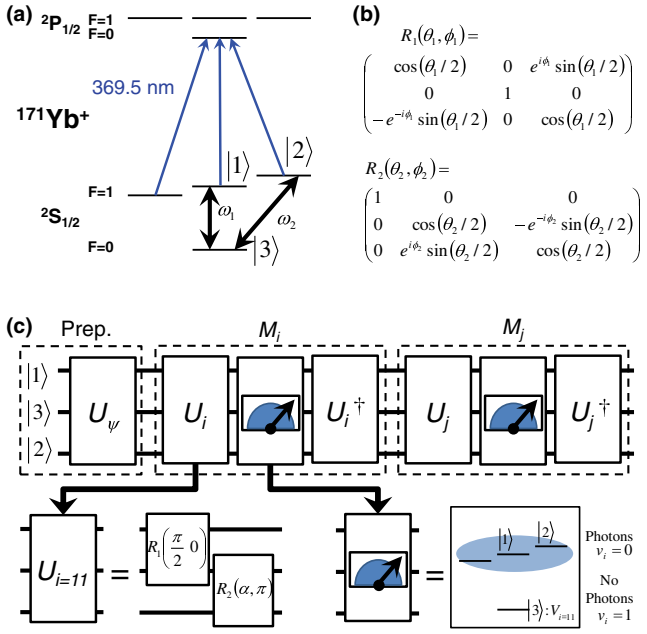

FIG. 2 (color online). The $^{171}Yb^+$ ion system and the measurement scheme. (a) The energy diagram of $^{171}Yb^+$. Qutrit states $|1\rangle$, $|2\rangle$, and $|3\rangle$ are mapped onto $|F = 1, m_F = 0\rangle$, $|F = 1, m_F = 1\rangle$, and $|F = 0, m_F = 0\rangle$ in the $S_{1/2}$ ground state manifold, respectively. The transition frequencies are $\omega_1 = (2\pi)12\,642.8213$ MHz and $\omega_2 = \omega_1 + (2\pi)7.6372$ MHz. The quantum state projected to $|1\rangle$ or $|2\rangle$ generates fluorescence, while the state collapsed to $|3\rangle$ does not generate photons. Therefore, we assign zero on the observable related to state $|3\rangle$ when we detect photons and one when no photons are detected. (b) The matrix representations of $R_1(\theta_1, \phi_1)$, $R_2(\theta_2, \phi_2)$ rotations, which are realized by applying microwave pulses with the frequencies of ω_1 and ω_2. Here θ_1, θ_2 and ϕ_1, ϕ_2 are controlled by the duration and the phase of the applied microwaves. (c) The sequential measurement scheme to detect the correlations $\langle V_iV_j \rangle$, where M_i and M_j denote the measurement boxes associated with the observables V_i and V_j, respectively. The detailed implementation is explained in the text.

the $^{171}Yb^{+}$ ion in the $S_{1/2}$ ground-state manifold, with $|1\rangle = |F = 1, m_F = 0\rangle$, $|2\rangle = |F = 1, m_F = 1\rangle$, and $|3\rangle = |F = 0, m_F = 0\rangle$, as shown in Fig. 2(a).

The experiment takes the following procedure: after 1 ms Doppler cooling, the state of the ion is initialized to $|3\rangle$ by 3 μs standard optical pumping [16]. The states for the test are coherently prepared by the microwaves ω_1 and ω_2 that are resonant to the transitions between $|1\rangle$ and $|3\rangle$, and between $|2\rangle$ and $|3\rangle$, respectively with high fidelity [17]. The pulse sequences for the preparations of different initial states are shown in Table I. The coherent rotations of the microwaves are represented by the matrices $R_1(\theta_1, \phi_1), R_2(\theta_2, \phi_2)$ shown in Fig. 2(b). Here θ_1, θ_2 and ϕ_1, ϕ_2 are controlled by the duration and the phase of the applied microwaves. The 2π times for both Rabi oscillations are adjusted to 29.5 μs, that is, the Rabi frequency $\Omega_{1,2} = (2\pi)33.9$ kHz. The separation $\omega_2 - \omega_1 = (2\pi)7.6372$ MHz with the magnetic field $B = 5.455$ G. The maximum probability of off-resonant excitation $\Omega^2/(\omega_2 - \omega_1)^2$ is about 1.6×10^{-5}, small enough to ensure the independence of each Rabi oscillation.

We measure the average of single observables, $\langle A_i \rangle$ in Eq. (1) or $\langle V_i \rangle$ in Eq. (2) by rotating the measurement axis $|v_i\rangle$ to the state $|3\rangle$ through microwave operation as shown in Fig. 2(c). Then we measure the probability of the state $P_{|3\rangle} = \langle V_i \rangle$, which gives $\langle A_i \rangle$ through $A_i = 1 - 2V_i$. The standard quantum jump detection based on the state-dependent fluorescence through a cycling transition can distinguish the $|F = 0\rangle$ level from the three $|F = 1\rangle$ levels. We observe on average 10 photons for the $|1\rangle$ or $|2\rangle$ states (referred to as the bright states) and basically no photon for the $|3\rangle$ state (referred to as the dark state) by collecting photons through an objective lens with high numerical aperture at the front side and backside of the ion trap system. We assign value 1 to V_i when no photons are detected and value 0 when photons are detected. Therefore, the probability $P_{|3\rangle}$ is obtained by dividing the number of no-photon events by the number of total repetitions. The state detection error rates for wrongly registering the state $|3\rangle$ and missing the state $|3\rangle$ are 0.5 and 1.5%, respectively, with the discrimination threshold set at $n_{\mathrm{ph}} = 1$.

To measure the correlations, we use the following relation: $\langle A_i A_j \rangle = \langle (1 - 2V_i)(1 - 2V_j) \rangle = 1 - 2\langle V_i \rangle - 2\langle V_j \rangle + 4\langle V_i V_j \rangle$, where $\langle V_i \rangle$ and $\langle V_j \rangle$ are obtained by the method described above. The correlation term $\langle V_i V_j \rangle$ is sequentially measured as shown in Fig. 2(c), composed of two consecutive measurement boxes M_i and M_j associated with the observables V_i and V_j, respectively. Each measurement box M_i is implemented by a unitary rotation U_i, followed by a measurement in the standard basis which detects projection to the state $|3\rangle$ and an inverse unitary rotation $U_i^{\dagger}$. The rotation U_i and thus the measurement box M_i is uniquely determined by the observable V_i and is implemented in the same way in the experiment when we measure the correlation of V_i with other compatible observables to assure context independence. The unitary U_i is realized with one or two microwave rotations and the corresponding pulse sequences for U_i $(i = 1, 2, \ldots, 13)$ are listed in Table I for all the 13 different observables V_i. As an example, we illustrate the measurement of the correlation $\langle V_i V_j \rangle$ with $i = 11$ in Fig. 2(c).

TABLE I. The pulse sequences for initial state preparation and measurement configurations for the 13 observables. We prepare the various initial states from a simple basis state via a superposition state to mixed states for the test of the state-independence of the inequalities (1) and (2). The state tomography results of the mixed states ρ_{10}, ρ_{11}, ρ_{12} are shown in Fig. 3. We rotate the three-dimensional coordinates to map an observable on the $|3\rangle$ state. Here $U_i (i = 1, 2, \ldots, 13)$ stands for unitary rotation for the projection observables A_i or V_i on the vectors $|v_i\rangle$ shown in Fig. 1(a) and α represents 0.392π. For the correlation measurements between the orthogonal observables shown as the edges of Fig. 1(b), we perform the sequential measurements described in Fig. 2(c). Note that the pulse sequences for the observables are conserved in the different experimental contexts.

Preparation sequences			Measurement sequences	
First	Second	Third	First	Second
ψ_1: $R_1(\pi, 0)$			$U_1 = R_1(\pi, \pi)$	
ψ_2: $R_2(\pi, 0)$			$U_2 = R_2(\pi, 0)$	
ψ_3: no rotation			$U_3 =$ no rotation	
ψ_4: $R_1(\pi/2, \pi)$			$U_4 = R_2(\pi/2, \pi)$	
ψ_5: $R_2(\pi/2, \pi)$			$U_5 = R_1(\pi/2, 0)$	
ψ_6: $R_1(\alpha, 0)$	$R_2(\pi/2, \pi)$		$U_6 = R_2(\pi, \pi)$	$R_1(\pi/2, \pi)$
ψ_7: $R_1(0.304\pi, 0)$			$U_7 = R_2(\pi/2, 0)$	
ψ_8: $R_2(0.288\pi, \pi)$	$R_1(0.533\pi, 0)$		$U_8 = R_1(\pi/2, \pi)$	
ψ_9: $R_1(\pi/2, \pi/2)$	$R_2(\pi, 0)$		$U_9 = R_2(\pi, 0)$	$R_1(\pi/2, \pi)$
ρ_{10}: $R_1(\pi/2, 0)$	$R_2(\pi, 0)$[0.5 ms]		$U_{10} = R_2(\pi/2, 0)$	$R_1(\alpha, 0)$
ρ_{11}: $R_1(\alpha, 0)$	$R_2(\pi/2, 0)$[0.5 ms]		$U_{11} = R_1(\pi/2, \pi)$	$R_2(\alpha, \pi)$
ρ_{12}: $R_1(\alpha, 0)$	$R_2(\pi/2, 0)$[1.0 ms]	$R_2(\pi, \pi)$[1.0 ms]$R_2(\pi, 0)$	$U_{12} = R_1(\pi/2, 0)$	$R_2(\alpha, \pi)$
			$U_{13} = R_1(\pi/2, \pi)$	$R_2(\alpha, 0)$

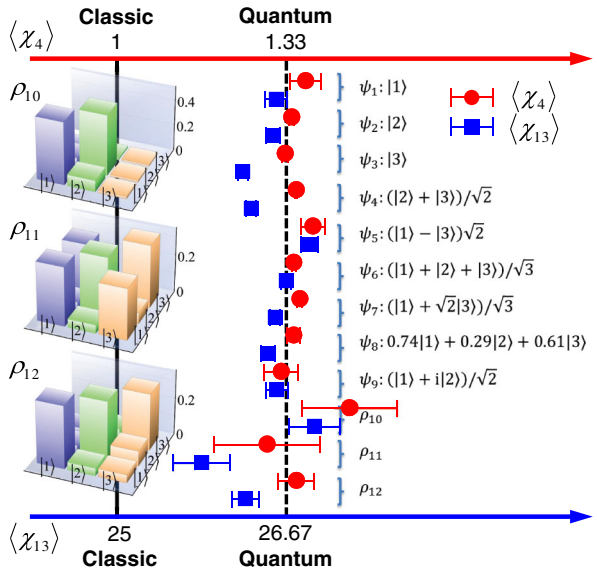

FIG. 3 (color online). State-independent test of KS inequalities $\langle\chi_4\rangle$ and $\langle\chi_{13}\rangle$ for a qutrit system. The inequalities (1) and (2) are examined with eleven different initial states including simple product states ψ_1 to ψ_3, superposition states at the axis of the observables ψ_4 to ψ_6, outside of the observables ψ_7 to ψ_9, and mixed states ψ_{10} to ψ_{12}. We measure the density matrix of all states by performing qutrit state tomography [19] and confirm the prepared states with an average fidelity 99.5% for the pure states ψ_1 to ψ_9. The mixed state fidelities are around 97%, shown in the figure. All raw measurements for $\langle\chi_{13}\rangle = 27.38(\pm 0.21)$ shown as blue filled squares violate the classical limit 25 by 11.2σ, confirming the quantum contextuality for various states. For each state, 480 000 realizations are used to obtain the $\langle\chi_{13}\rangle$. For the inequality (2), the average value of all measured initial states is $\langle\chi_4\rangle = 1.35(\pm 0.04)$.

For the last terms in the equality (1), we apply similar methods as described above. The correlations $-\langle A_i A_j A_k\rangle$ are expanded to $-1 + 2\langle V_i\rangle + 2\langle V_j\rangle + 2\langle V_k\rangle - 4\langle V_i V_j\rangle - 4\langle V_j V_k\rangle - 4\langle V_k V_i\rangle + 8\langle V_i V_j V_k\rangle$. We can ignore the terms $\langle V_i V_j V_k\rangle$ because they should not have negative values and the inequality without these terms should be bounded by the same value, 25. Note that we do not discard any measured data to construct the inequality, which ensures that the experiment requires no fair-sampling assumption and thus is free from the detection efficiency loophole.

We perform the measurements of 24 correlations of compatible observables with exchanged order and the average values of the 13 observables under a given initial state. We repeat the same measurements 10 000 times for the same observable, which result in 480 000 repetitions for one initial state. To show that the inequalities (1) and (2) can be violated independent of the system state, we prepare 12 different initial states as shown in Table I and Fig. 3 and repeat the measurements described in Fig. 2(c) and Table I. We observe the fidelities of the prepared states to be on average 98%.

From our observation, the inequalities (1) and (2) are clearly violated for all the input states that we tested, including mixed states as summarized in Fig. 3. The average of $\langle\chi_{13}\rangle = 27.38(\pm 0.21)$ and $\langle\chi_4\rangle = 1.35(\pm 0.04)$, significantly larger than the limits set by noncontextual hidden variable models. For some of the input states, $\langle\chi_4\rangle$ and $\langle\chi_{13}\rangle$ are even larger than the quantum bounds, but this is of no physical significance as the results are within the error bar.

In summary, we have observed violation of the KS inequality for the indivisible qutrit system using a single trapped ion, closing the detection efficiency loophole for this fundamental system that manifests quantum contextuality. The measurement results are in agreement with quantum mechanical predictions and violate the bounds set by any noncontextual hidden variable models by a significant margin. The compatibility loophole of the sequential measurements could be handled in the extended contextual models [18].

We thank Hyunchul Nha and Sewan Ji for helpful discussion and Emily Lichko for careful reading of the manuscript. This work was supported by the National Basic Research Program of China under Grants No. 2011CBA00300 (No. 2011CBA00301), the National Natural Science Foundation of China 61073174, 61033001, 61061130540. K. K. acknowledges the support from the Thousand Young Talents program.

*kimkihwan@mail.tsinghua.edu.cn

[1] S. Kochen and E. P. Specker, J. Math. Mech. **17**, 59 (1967).
[2] J. S. Bell, Rev. Mod. Phys. **38**, 447 (1966).
[3] G. Kirchmair, F. Zähringer, R. Gerritsma, M. Kleinmann, O. Gühne, A. Cabello, R. Blatt, and C. F. Roos, Nature (London) **460**, 494 (2009).
[4] E. Amselem, M. Rådmark, M. Bourennane, and A. Cabello, Phys. Rev. Lett. **103**, 160405 (2009).
[5] H. Bartosik, J. Klepp, C. Schmitzer, S. Sponar, A. Cabello, H. Rauch, and Y. Hasegawa, Phys. Rev. Lett. **103**, 040403 (2009).
[6] O. Moussa, C. A. Ryan, D. G. Cory, and R. Laflamme, Phys. Rev. Lett. **104**, 160501 (2010).
[7] N. D. Mermin, Phys. Rev. Lett. **65**, 3373 (1990).
[8] A. Peres, J. Phys. A **24**, L175 (1991).
[9] A. Cabello, Phys. Rev. Lett. **101**, 210401 (2008).
[10] A. A. Klyachko, M. A. Can, S. Binicioğlu, and A. S. Shumovsky, Phys. Rev. Lett. **101**, 020403 (2008).
[11] S. Yu and C. H. Oh, Phys. Rev. Lett. **108**, 030402 (2012).
[12] A. Cabello, arXiv:1112.5149.
[13] R. Lapkiewicz, P. Li, C. Schaeff, N. K. Langford, S. Ramelow, M. Wieśniak, and A. Zeilinger, Nature (London) **474**, 490 (2011).
[14] C. Zu, Y.-X. Wang, D.-L. Deng, X.-Y. Chang, K. Liu, P.-Y. Hou, H.-X. Yang, and L.-M. Duan, Phys. Rev. Lett. **109**, 150401 (2012).
[15] A. Cabello, C. Budroni, O. Gühne, M. Kleinmann, and J. Å. Larsson, Phys. Rev. Lett. **109**, 250402 (2012).

[16] S. Olmschenk, K. C. Younge, D. L. Moehring, D. N. Matsukevich, P. Maunz, and C. Monroe, Phys. Rev. A **76**, 052314 (2007).

[17] K. R. Brown, A. C. Wilson, Y. Colombe, C. Ospelkaus, A. M. Meier, E. Knill, D. Leibfried, and D. J. Wineland, Phys. Rev. A **84**, 030303(R) (2011).

[18] O. Gühne, M. Kleinmann, A. Cabello, J. A. Larsson, G. Kirchmair, F. Zähringer, R. Gerritsma, and C. F. Roos, Phys. Rev. A **81**, 022121 (2010).

[19] R. T. Thew, K. Nemoto, A. G. White, and W. J. Munro, Phys. Rev. A **66**, 012303 (2002).